J|A|C|S
ARTICLES
Published on Web 03/09/2005

Structure of and Competitive Adsorption in Alkyl Dicarbamate Two-Dimensional Crystals

Kibum Kim, Katherine E. Plass, and Adam J. Matzger*

Contribution from the Department of Chemistry and Macromolecular Science and Engineering Program, University of Michigan, 930 North University, Ann Arbor, Michigan 48109-1055

Received November 18, 2004; E-mail: matzger@umich.edu

Abstract: The potential for relatively minor structural changes to dramatically impact materials properties is one of the primary obstacles to achieving the rational design of functional materials. For example, having an odd versus an even number of carbons between functional groups in polymers can cause large variation in melting point and mechanical properties. This odd−even effect is especially pronounced in hydrogen-bonded polymers and oligomers. To shed light on the structural basis of this phenomenon, physisorbed monolayers and single crystals of alkyl dicarbamates were investigated by scanning tunneling microscopy and X-ray diffraction, respectively. The related two- and three-dimensional crystal structures both demonstrated a clear odd−even effect in packing geometry. The differing accommodation of intermolecular interactions between odd and even packing motifs was directly related to the melting point trends and further dissected through computation. In addition, these oligomers displayed unusual competitive adsorption behavior; the relative preference for adsorption of a smaller species from a binary solution was increased compared to alkanes. These results were explained in the context of hydrogen bond density effects that arise due to competition for a limited substrate surface area. This study provides a model for understanding oligourethane surface coatings and demonstrates the importance of molecular structure and hydrogen bonding in determining adsorption behavior.

Introduction

The exceptional properties of many polymers and oligomers are ascribed to the formation of cooperative hydrogen-bonding networks. This holds for certain polyurethanes, polyamides, and polyureas, many of which are used as surface coatings.[1,2] At an interface with a dissimilar material, deviation from the bulk structure occurs to an extent that depends dramatically on the nature of the substrate-adsorbed layer interaction.[3] Despite the profound importance of such phenomena in applications such as controlling adhesion and filler compatibility, few techniques are capable of probing these interfaces with atomic detail. Scanning tunneling microscopy (STM) has proven a successful approach for observing molecules adsorbed on metals and semiconductors.[4,5] Inasmuch as these atomically flat substrates are models for the types of materials coated with polymers and oligomers industrially, employing STM on model systems is capable of providing substantial insight into the interfacial structure of many technologically important systems. Combining such information with bulk structural data derived from crystallography further elucidates the extent of restructuring possible for polymers and oligomers contacting surfaces.[6]

Polymeric and oligomeric urethanes, substances which contain the carbamate functional group, have exceptional properties arising from strong hydrogen bonding. Because of their good adhesion and flexibility, these materials are employed as major components in applications such as magnetic recording media, antistatic coatings, and paints.[1] One filler employed for tinting and imparting electrical conductivity to polyurethane composites is carbon black. An atomically flat substrate which mimics the surface properties of this filler is highly oriented pyrolytic graphite (HOPG). We have recently demonstrated that mono-

(1) Oertel, G.; Abele, L. *Polyurethane Handbook: Chemistry, Raw Materials, Processing, Application, Properties*, 2nd ed.; Hanser: New York, 1994; Wirpsza, Z. *Polyurethanes: Chemistry, Technology and Applications*; Ellis Horwood: New York, 1993.
(2) Cowie, J. M. G. *Polymers: Chemistry & Physics of Modern Materials*, 2nd ed.; Nelson Thornes Ltd.: Cheltenham, 1991.
(3) Everett, D. H.; Findenegg, G. H. *Nature* **1969**, *223*, 52−53. Kern, H.; Rybinski, W. V.; Findenegg, G. H. *J. Colloid Interface Sci.* **1977**, *59*, 301−307. Castro, M. A.; Clarke, S. M.; Inaba, A.; Thomas, R. K. *J. Phys. Chem. B* **1997**, *101*, 8878−8882. Samori, P.; Francke, V.; Enkelmann, V.; Müllen, K.; Rabe, J. P. *Chem. Mater.* **2003**, *15*, 1032−1039. Grave, C.; Lentz, D.; Schafer, A.; Samori, P.; Rabe, J. P.; Franke, P.; Schluter, A. D. *J. Am. Chem. Soc.* **2003**, *125*, 6907−6918. Smith, D. P. E.; Horber, H.; Gerber, C.; Binnig, G. *Science* **1989**, *245*, 43−45. Mu, Z. C.; Kong, J. F.; Wang, Y.; Ye, L.; Yang, G. D.; Zhang, X. *ChemPhysChem* **2004**, *5*, 202−208.
(4) Wiesendanger, R. *Scanning Probe Microscopy and Spectroscopy: Methods and Applications*; Cambridge University Press: New York, 1994. Chen, C. J. *Introduction to Scanning Tunneling Microscopy*; Oxford University Press: New York, 1993. Giancarlo, L. C.; Flynn, G. W. *Annu. Rev. Phys. Chem.* **1998**, *49*, 297−336. Giancarlo, L. C.; Flynn, G. W. *Acc. Chem. Res.* **2000**, *33*, 491−501. De Feyter, S.; De Schryver, F. C. *Chem. Soc. Rev.* **2003**, *32*, 139−150. Hamers, R. J. *J. Phys. Chem.* **1996**, *100*, 13103−13120. France, C. B.; Schroeder, P. G.; Forsythe, J. C.; Parkinson, B. A. *Langmuir* **2003**, *19*, 1274−1281.
(5) De Feyter, S.; Larsson, M.; Schuurmans, N.; Verkuijl, B.; Zoriniants, G.; Gesquière, A.; Abdel-Mottaleb, M. M.; van Esch, J.; Feringa, B. L.; van Stam, J.; De Schryver, F. *Chem.-Eur. J.* **2003**, *9*, 1198−1206.
(6) Azumi, R.; Götz, G.; Bäuerle, P. *Synth. Met.* **1999**, *101*, 569−572. Azumi, R.; Götz, G.; Debaerdemaeker, T.; Bäuerle, P. *Chem.-Eur. J.* **2000**, *6*, 735−744. Mena-Osteritz, E.; Meyer, A.; Langeveld-Voss, B. M. W.; Janssen, R. A. J.; Meijer, E. W.; Bäuerle, P. *Angew. Chem., Int. Ed.* **2000**, *39*, 2680−2684. Grevin, B.; Rannou, P.; Payerne, R.; Pron, A.; Travers, J. P. *J. Chem. Phys.* **2003**, *118*, 7097−7102. Stecher, R.; Gompf, B.; Munter, J. S. R.; Effenberger, F. *Adv. Mater.* **1999**, *11*, 927−931. Holland, N. B.; Qiu, Y. X.; Ruegsegger, M.; Marchant, R. E. *Nature* **1998**, *392*, 799−801.

Chart 1. Structure of Alkyl Dicarbamates Synthesized and Studied[a]

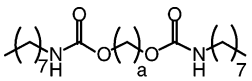

8-12-8 dicarbamate a=12
8-9-8 dicarbamate a=9
8-8-8 dicarbamate a=8
8-5-8 dicarbamate a=5
8-4-8 dicarbamate a=4

[a] The **8-12-8**, **8-9-8**, and **8-8-8 dicarbamates** were imaged by STM, and **8-5-8** and **8-4-8 dicarbamates** were investigated by single-crystal X-ray diffraction.

carbamates, which resemble a segment of the polyurethane structure, order spontaneously on HOPG to form monolayers composed of densely packed two-dimensional crystalline domains.[7,8] Furthermore, a given molecule can produce different geometries of packing and the evolution of these structures was found to be time dependent. The findings suggested that the organization of poly- and oligourethanes might be also affected by small changes in their molecular structure. To provide a better understanding of this class of materials in surface-coating applications, two- and three-dimensional crystal structures of dicarbamates were investigated by STM and X-ray diffraction, respectively. The effect of molecular structure on the packing geometry in two- and three-dimensions was clearly demonstrated and an odd−even effect was observed. In addition, the competitive adsorption between two dicarbamates was studied with STM and the role of hydrogen bonding in determining the relative preference of monolayer formation was demonstrated.

Experimental Section

Scanning Tunneling Microscopy. A drop of 1-phenyloctane (Acros Organics) solution containing the compound to be imaged was placed on freshly cleaved HOPG (SPI-1 grade, Structure Probe Inc.) to obtain a self-assembled monolayer at the solution−solid interface. A nearly saturated solution was used to obtain the STM images of alkyl dicarbamates except when competitive monolayer formation was performed. The solutions used for competition experiments were composed of two alkyl dicarbamates in varying mole fractions, and the total concentration of alkyl dicarbamates in the solution was maintained at 0.30−0.80 mg/mL. A Nanoscope E STM (Digital Instruments) was used for all imaging. The tips were fabricated from Pt/Ir wire (Pt/Ir = 80/20%, California Fine Wire) by mechanical cutting and the quality of the tips was verified by scanning bare HOPG prior to imaging. STM imaging was performed under ambient conditions with typical settings of between 200 and 400 pA of current and 600−1000 mV of bias voltage (sample positive).

Synthesis. All solvents were purchased from Fisher Scientific except ethanol (Pharmco). THF was purified by passage through activated alumina columns. All reagents were used as received and were purchased from Acros Organics except dibutyltin dilaurate and 1,12-dodecanediol (Sigma-Aldrich Co.). Carbamate names are derived by designating the number of carbons in the alkyl chain derived from the isocyanate and alcohol. For example, a dicarbamate synthesized from two molecules of octyl isocyanate and 1,12-dodecanediol is designated as the **8-12-8 dicarbamate** (Chart 1). In a typical synthesis, octyl isocyanate was added to a mixture of a diol and dibutyltin dilaurate. The mixture was heated for several hours under a nitrogen atmosphere and the pure product was obtained by recrystallization. Detailed synthetic procedures and full characterization for each alkyl dicarbamate are provided in the Supporting Information.

Molecular Modeling. Molecular mechanics modeling was carried out with the COMPASS force field[9] as implemented in Cerius[2] version 4.2 from Accelrys Inc. In a typical modeling experiment, the optimized geometry of an isolated single molecule was obtained in the extended chain conformation, followed by the construction and optimization of a three-dimensional periodic model. The periodic model was based on a monoclinic unit cell with unique *c*-axis and was built in a way such that a layer of the model through the $a-b$ plane represents the arrangement of molecules observed by the STM. The non-90° unit cell angle is in the $a-b$ plane. The *c*-axis of the model, which is the distance between molecular layers, was set at 30 Å and was fixed during structure optimization. The length of the *c*-axis was verified not to affect the computational result by calculating the energy of the structure with different lengths of this axis.

X-ray Crystallography. Diffraction data were obtained using a Bruker SMART CCD-based X-ray diffractometer equipped with an LT-2 low-temperature device and a Mo Kα source ($\lambda = 0.71073$ Å). The structures were solved by direct methods (SIR2002)[10] and refined using SHELXL-97[11] as implemented by WinGX.[12] Hydrogen atoms have fixed thermal parameters and riding coordinates. Full details of the X-ray structure determination are provided in the Supporting Information.

Results and Discussion

To investigate the relationship between molecular structure and packing geometry of alkyl dicarbamate two-dimensional crystals, **8-12-8**, **8-9-8**, and **8-8-8 dicarbamates** (Chart 1) were synthesized and investigated by STM. Long alkyl chains promote monolayer formation and improve STM resolution by immobilizing the molecules through close packing.[13] The lengths of the alkyl chains were selected on the basis of the ease of monolayer formation and, in the case of the central alkyl segment, to study the odd−even effect. To elucidate the packing structure of alkyl dicarbamates in three-dimensional crystals, **8-4-8** and **8-5-8 dicarbamates** were synthesized and investigated by single-crystal X-ray diffraction.

STM Imaging of Alkyl Dicarbamate Monolayers. Figure 1a shows an STM image of a monolayer of **8-12-8 dicarbamate** formed on HOPG from a phenyloctane solution. An energy-minimized periodic model is overlaid to aid visualization of the molecular geometry and packing structure in this two-dimensional crystal. The columnar structure accommodates both hydrogen bonding between the carbamate functional groups and van der Waals interaction between the alkyl chains within a column. The alkyl groups have an extended chain conformation that is typically observed in physisorbed self-assembled monolayers of molecules with long alkyl chains.[14] The unit cell parameters obtained from measurement of the STM images and by computation employing molecular mechanics show close agreement (Table 1). The molecule is bent around the carbamate functional group (154 ± 8°); this geometry is also found in the

(7) Kim, K.; Plass, K. E.; Matzger, A. J. *Langmuir* **2003**, *19*, 7149−7152.
(8) Kim, K.; Plass, K. E.; Matzger, A. J. *Langmuir* **2005**, *21*, 647−655.
(9) Sun, H. *J. Phys. Chem. B* **1998**, *102*, 7338−7364.
(10) Burla, M. C.; Camalli, M.; Carrozzini, B.; Cascarano, G. L.; Giacovazzo, C.; Polidori, G.; Spagna, R. *J. Appl. Crystallogr.* **2003**, *36*, 1103.
(11) Sheldrick, G. M. *SHELXL-97*; University of Göttingen: Göttingen, 1997.
(12) Farrugia, L. J. *J. Appl. Crystallogr.* **1999**, *32*, 837−838.
(13) Qiu, X. H.; Wang, C.; Zeng, Q. D.; Xu, B.; Yin, S. X.; Wang, H. N.; Xu, S. D.; Bai, C. L. *J. Am. Chem. Soc.* **2000**, *122*, 5550−5556. Qiu, X. H.; Wang, C.; Yin, S. X.; Zeng, Q. D.; Xu, B.; Bai, C. L. *J. Phys. Chem. B* **2000**, *104*, 3570−3574.
(14) McGonigal, G. C.; Bernhardt, R. H.; Yeo, Y. H.; Thomson, D. J. *J. Vac. Sci. Technol., B* **1991**, *9*, 1107−1110. Rabe, J. P.; Buchholz, S. *Makromol. Chem., Macromol. Symp.* **1991**, *50*, 261−268. Claypool, C. L.; Faglioni, F.; Goddard, W. A.; Gray, H. B.; Lewis, N. S.; Marcus, R. A. *J. Phys. Chem. B* **1997**, *101*, 5978−5995. Cincotti, S.; Rabe, J. P. *Appl. Phys. Lett.* **1993**, *62*, 3531−3533. Zhang, H. M.; Xie, Z. X.; Mao, B. W.; Xu, X. *Chem.-Eur. J.* **2004**, *10*, 1415−1422.

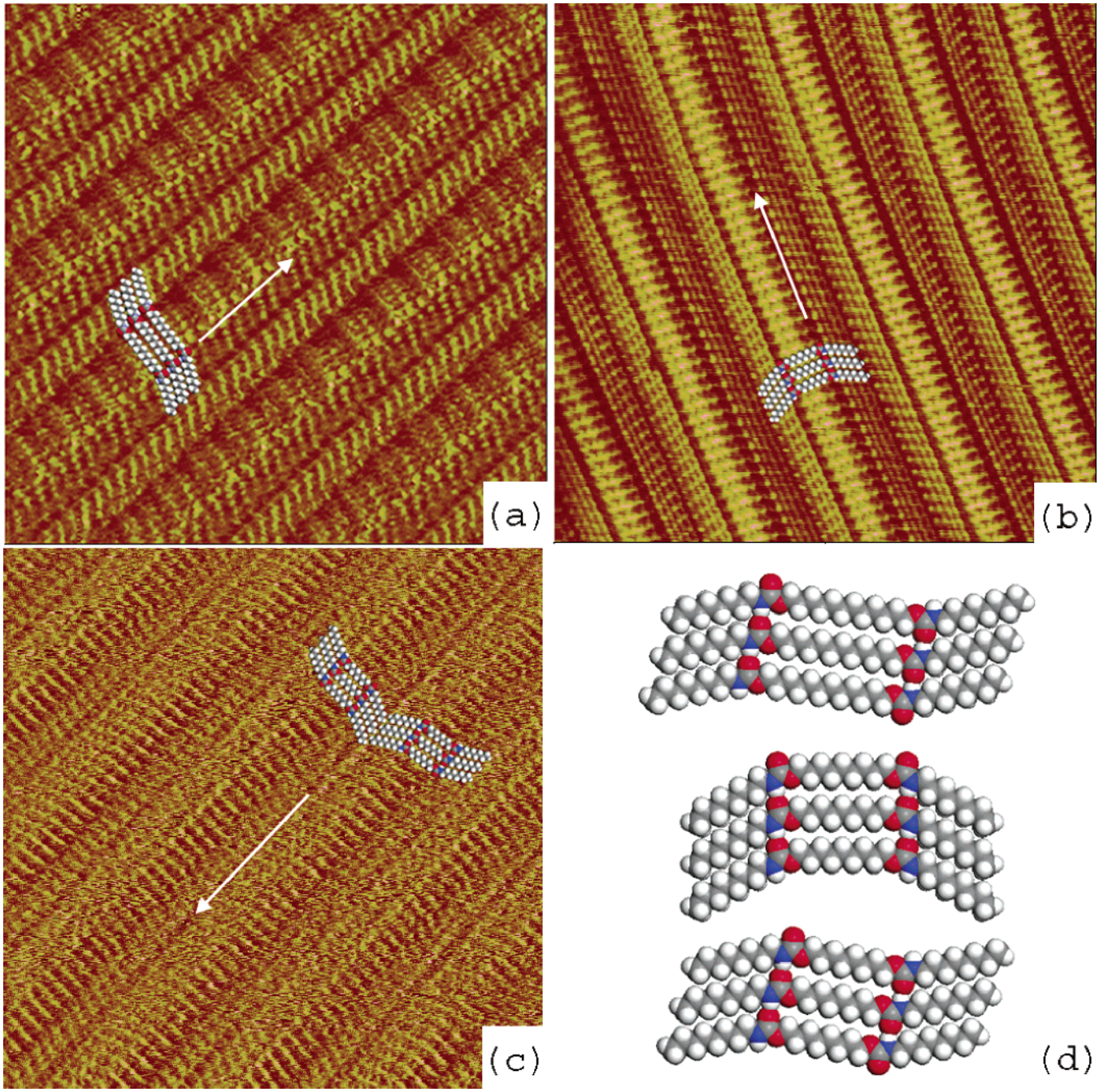

Figure 1. STM images (20 × 20 nm^2) of alkyl dicarbamate physisorbed monolayers. (a) The **8-12-8 dicarbamate** has an anti configuration of the two terminal alkyl chains due to the even number of carbons in the central alkyl group. An optimized molecular model is overlaid to aid visualization of the molecular conformation. White arrows designate the column direction, which is nearly perpendicular with respect to the central alkyl chain and forms an acute angle with the two terminal alkyl chains. (b) The **8-9-8 dicarbamate** has a syn configuration of the two terminal alkyl chains due to the odd number of carbons in the central alkyl group. (c) STM image of **8-8-8 dicarbamate** showing an anti configuration of the two terminal alkyl chains as in the case of **8-12-8 dicarbamate**. (d) Enlarged molecular models of **8-12-8**, **8-9-8**, and **8-8-8 dicarbamates** (from the top).

three-dimensional crystal structure of an alkyl carbamate[15] as well as in monocarbamate monolayers.[7,8] The central and terminal alkyl chains display a slightly different image contrast, which likely arises from the difference in topography of the two alkyl chains.[8] The two terminal alkyl chains point in opposite directions, giving rise to an anti geometry. The column direction, designated with a white arrow in Figure 1a, is approximately perpendicular to the central alkyl segment.

Compared to **8-12-8 dicarbamate**, **8-9-8 dicarbamate** is slightly shorter and possesses an odd number of carbons between carbamate functional groups. These compounds are otherwise identical, and therefore comparison of the two-dimensional packing structure of **8-9-8** and **8-12-8 dicarbamates** enables isolation of the effect of altering the parity of the number of carbons in the central alkyl chain. The STM image in Figure 1b shows the molecular geometry and the packing structure of **8-9-8 dicarbamate**. The columnar structure and the bent molecular geometry observed in the monolayer of **8-12-8 dicarbamate** are also found in this monolayer. In contrast to **8-12-8 dicarbamate**, the two terminal alkyl chains are pointing

(15) Alimova, L. L.; Atovmyan, E. G.; Filipenko, O. S. *Kristallografiya* **1987**, *32*, 97−101.

Table 1. Experimental and Computed Unit Cell Parameters and Angle around the Carbamate Group for the Monolayers of Alkyl Dicarbamates Investigated

dicarbamate		*a* (nm)	*b* (nm)	α (°)	carbamate angle (°)[a]
8-12-8	STM	4.4 ± 0.2	0.50 ± 0.02	86 ± 4	154 ± 8
	model	4.18	0.50	83	161
8-9-8	STM	3.9 ± 0.2	0.50 ± 0.01	86 ± 3	157 ± 7
	model	3.77	0.50	86	156
8-8-8	STM	3.8 ± 0.3	0.50 ± 0.02	89 ± 3	158 ± 4
	model	3.64	0.50	90	161

[a] The carbamate angle is the angle adopted between the two alkyl chains around the carbamate functional group.

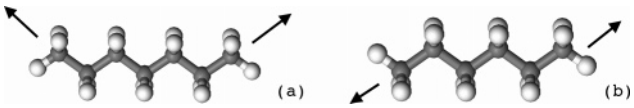

Figure 2. Odd−even effect due to the zigzag shape of the alkyl backbone. (a) The two methyl groups at the end of heptane have a syn conformation, whereas (b) the two methyl groups at the end of hexane have an anti conformation.

in the same direction, a syn geometry. Because the central alkyl chain is in an extended (zigzag) conformation and horizontal to the graphite surface, odd numbers of carbons in the backbone result in a change in the relative direction of the two terminal alkyl chains when compared to molecules with an even number of carbons (Figure 2). The column direction is nearly perpendicular to the central alkyl chain as observed in **8-12-8 dicarbamate** and forms an angle of ∼60° with the terminal alkyl chains due to the bent geometry about the carbamate functional group. The observed and computed unit cell parameters of this two-dimensional crystal show close agreement (Table 1).

Shortening the central alkyl chain further results in **8-8-8 dicarbamate**. The STM image of this even-numbered dicarbamate monolayer is presented in Figure 1c. It has the same bent conformation and anti configuration of the two terminal alkyl groups that were observed in the monolayer of **8-12-8 dicarbamate**. The packing structure within a molecular column is similar between the two even-numbered alkyl dicarbamates. A pseudo-glide plane relationship, where molecules in two neighboring columns are related by reflection then translation within the column, is most commonly adopted, although the simple translational symmetry that is the dominant packing motif in **8-12-8 dicarbamate** also occurs. These two packing motifs are mixed randomly within the monolayer of **8-8-8 dicarbamate** and computation by molecular mechanics shows that they are very close in energy (<0.2 kcal/mol). The resolution of STM images of **8-8-8 dicarbamate** was generally low compared to the resolution of **8-12-8 dicarbamate** despite repeated experiments under various conditions. This may result from increased mobility of this relatively small molecule on the surface.

Two-Dimensional vs Three-Dimensional Crystal Structure of Alkyl Dicarbamates. STM imaging of physisorbed monolayers gives an exquisitely detailed view of molecular organization on a substrate. However, this arrangement may differ substantially from that in the solid state. For carboxylic acids,[16,17] alcohols,[17,18] and ureas,[5,19,20] similar packing motifs in two- and three-dimensional crystals are observed. To investigate the structural similarity between two- and three-dimensional alkyl dicarbamate crystals, the STM images were compared to the available three-dimensional crystal structures of analogous compounds. Although there are a number of crystal structures reported for carbamates, molecules containing other functional groups were not employed for comparison in order to ensure that the packing structure is determined primarily by the intermolecular interaction of alkyl and carbamate functional groups. Prior to this study, there was only one reported crystal structure of an alkyl dicarbamate[15] in the Cambridge Structural Database (CSD). This molecule, *N*,*N*′-hexanediyl-bis-carbamic acid bis-decyl ester, has the opposite orientation of the carbamate functional groups in the molecule compared to the alkyl dicarbamates in this study. In other words, this molecule has nitrogens connected to the central alkyl chain and oxygens on the terminal alkyl chain whereas this relationship is reversed in the alkyl dicarbamates discussed here. This lone example does not provide sufficient information to confidently compare two- and three-dimensional packing motifs particularly for the molecule with an odd number of carbons. This led us to determine the single-crystal structure of two alkyl dicarbamates. Due to the difficulty associated with obtaining single crystals suitable for X-ray structure analysis for the compounds employed in STM imaging, the crystal structures of **8-4-8** and **8-5-8 dicarbamates** were determined and compared instead. Although these molecules are too small to provide high-resolution STM images, the selection of these compounds for X-ray crystallography is justified by the observation that a homologous series of molecules often adopt similar molecular geometry and packing motifs within an odd or even series. For example, odd-numbered diols such as pentanediol, heptanediol, and nonanediol crystallize in the space group $P2_12_12_1$, whereas even-numbered diols such as butanediol, hexanediol, and octanediol adopt the space group $P2_1/n$.[21] The formation of the same packing motif within a series of isostructural molecules is also found for diacids[22] and dithiols[23] albeit with a complication due to polymorphism in the case of diacids.

In the solid state, both **8-4-8** and **8-5-8 dicarbamates** have a lamellar structure that accommodates intermolecular hydrogen bonding of carbamate functional groups within the lamellae (Figure 3a). The layers extracted from the three-dimensional crystal structures clearly illustrate the presence of a common packing motif between the two- and the three-dimensional crystals. The lamellae of **8-4-8 dicarbamate** are isostructural to the monolayer of **8-8-8** and **8-12-8 dicarbamates**. The molecule has a bent geometry and the two terminal alkyl chains bear an anti relationship. The *a*-axis coincides with the molecular column direction and the central alkyl chain is almost perpendicular (86°) to this axis. The similarity in packing structure

(16) Miura, A.; De Feyter, S.; Abdel-Mottaleb, M. M. S.; Gesquière, A.; Grim, P. C. M.; Moessner, G.; Sieffert, M.; Klapper, M.; Müllen, K.; De Schryver, F. C. *Langmuir* **2003**, *19*, 6474−6482. Hoeppener, S.; Chi, L. F.; Fuchs, H. *Chemphyschem* **2003**, *4*, 494−498; Olson, J. A.; Bühlmann, P. *Anal. Chem.* **2003**, *75*, 1089−1093.

(17) Wintgens, D.; Yablon, D. G.; Flynn, G. W. *J. Phys. Chem. B* **2003**, *107*, 173−179.

(18) Cai, Y. U.; Bernasek, S. L. *J. Am. Chem. Soc.* **2003**, *125*, 1655−1659.

(19) De Feyter, S.; Grim, P. C. M.; van Esch, J.; Kellogg, R. M.; Feringa, B. L.; De Schryver, F. C. *J. Phys. Chem. B* **1998**, *102*, 8981−8987.

(20) Gesquière, A.; Abdel-Mottaleb, M. M. S.; De Feyter, S.; De Schryver, F. C.; Schoonbeek, F.; van Esch, J.; Kellogg, R. M.; Feringa, B. L.; Calderone, A.; Lazzaroni, R.; Brédas, J. L. *Langmuir* **2000**, *16*, 10385−10391.

(21) Thalladi, V. R.; Boese, R.; Weiss, H. C. *Angew. Chem., Int. Ed.* **2000**, *39*, 918−922.

(22) Thalladi, V. R.; Nusse, M.; Boese, R. *J. Am. Chem. Soc.* **2000**, *122*, 9227−9236.

(23) Thalladi, V. R.; Boese, R.; Weiss, H. C. *J. Am. Chem. Soc.* **2000**, *122*, 1186−1190.

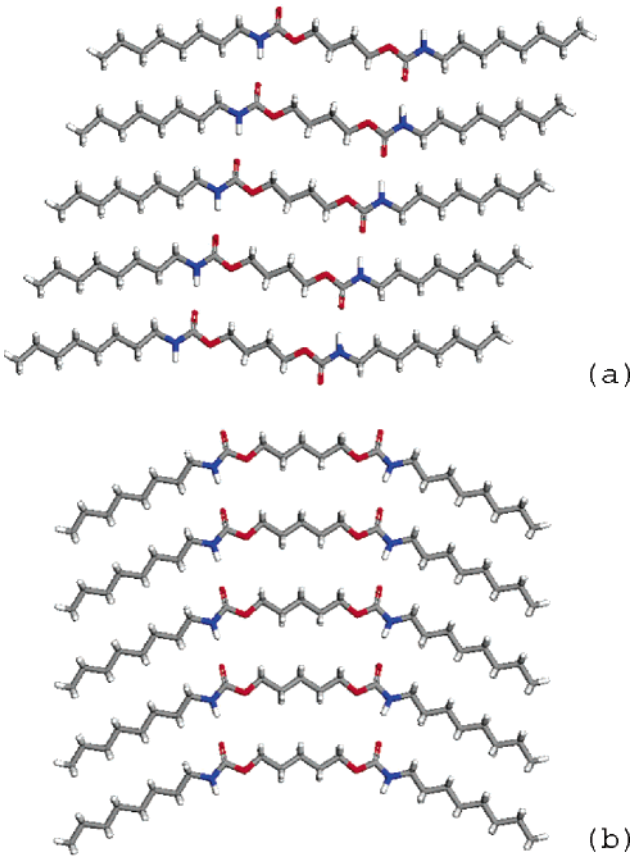

Figure 3. Crystal structure of **8-4-8 dicarbamate** and **8-5-8 dicarbamates** showing the layered structure of these crystals and close resemblance between the two- and three-dimensional crystal structure of alkyl dicarbamates. (a) A slice of the three-dimensional crystal structure of **8-4-8 dicarbamate** along the (042) plane. The arrangement of molecules in the slice is analogous to the monolayer of **8-12-8 dicarbamate**. (b) A slice of the three-dimensional crystal structure of **8-5-8 dicarbamate** along the (02−2) plane. Note the resemblance of the molecular conformation and arrangement to **8-9-8 dicarbamate** monolayer.

between the two- and three-dimensional crystals found for the alkyl dicarbamates with even numbers of carbons persists for the odd series. A lamellae taken from the crystal structure of **8-5-8 dicarbamate** (Figure 3b) illustrates the syn relationship between the two terminal alkyl chains and the perpendicular geometry between the central alkyl chain and the molecular column direction that were observed in the monolayer of **8-9-8 dicarbamate**. Therefore, the two odd alkyl dicarbamates are isostructural in their two- and three-dimensional crystals indicating that only minor modification of molecular geometry occurs from the bulk structure when carbamates contact a graphitic surface.

Odd−Even Effect in Alkyl Dicarbamate Crystals. The systematic change in solid-state properties depending on the parity of the number of carbons in a molecule, the odd−even effect, has been observed for many classes of compounds. Illustrative examples include α,ω-alkane diols,[21] α,ω-alkane diacids,[22] and *n*-alkanes.[24] Changes in packing geometry ascribed to the odd−even effect have been observed in both two-[5,19,25] and three-dimensional crystals.[21−24] In addition, this phenomenon is evident in the physical property variations in polymeric materials including polyamides,[26] polyesters,[27] and

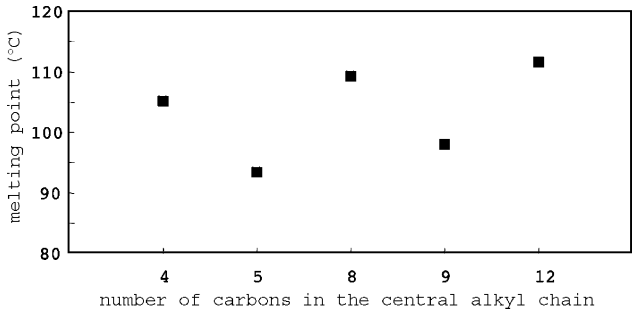

Figure 4. Melting points of alkyl dicarbamates. The vertical axis denotes the melting point (°C) and the horizontal axis is the number of carbons in the central alkyl chain. For example, the 4 indicates **8-4-8 dicarbamate**. The odd-numbered dicarbamates display lower melting points compared to the even-numbered dicarbamates.

liquid crystalline polymers.[28,29] These differences are often observed during thermal analysis or through experiments such as NMR or IR spectroscopy.[29,30] The STM images of **8-8-8**, **8-9-8**, and **8-12-8 dicarbamates** and the crystal structures of **8-4-8** and **8-5-8 dicarbamates** suggest the structural origin of these phenomena for polyurethanes by demonstrating the difference in packing structure between odd and even dicarbamates.

The parity of the number of carbons between carbamate groups in the alkyl backbone affects the organization of molecules on surfaces as well as in three-dimensional space, which in turn changes the solid-state properties of alkyl dicarbamates. The melting points of even-numbered alkyl dicarbamates increase slightly with the molecular weight, from 105 °C for **8-4-8 dicarbamate**, to 109 °C for **8-8-8 dicarbamate**, to 111 °C for **8-12-8 dicarbamate**. For a similar molecular weight, the odd-numbered alkyl dicarbamates display significantly lower melting points than those with even numbers of carbons (Figure 4). The melting points of **8-5-8 dicarbamate** and **8-9-8 dicarbamate** are lower than those of the alkyl dicarbamates with a similar but even number of carbons by more than 10 °C. There is a 12 °C difference between **8-5-8** and **8-4-8 dicarbamates** and an 11 °C difference between **8-9-8** and **8-8-8 dicarbamates**, demonstrating a marked odd−even effect. Lattice energy calculations (Table 2) suggest a possible explanation for the melting point lowering in the odd-numbered alkyl dicarbamates. The intermolecular interaction in **8-9-8 dicarbamate** is smaller than in **8-8-8** or **8-12-8 dicarbamate** mainly due to the decrease in electrostatic interaction. For alkyl carbamates, hydrogen bonding between functional groups is the primary contributor to the electrostatic interaction whereas van der Waals interaction is mostly due to the alkyl chains.[8] In the case of

(24) Boese, R.; Weiss, H. C.; Blaser, D. *Angew. Chem., Int. Ed.* **1999**, *38*, 988−992.
(25) Izumi, H.; Yamagami, S.; Futamura, S.; Nafie, L. A.; Dukor, R. K. *J. Am. Chem. Soc.* **2004**, *126*, 194−198. Taki, S.; Kai, S. *Jpn. J. Appl. Phys., Part 1* **2001**, *40*, 4187−4192. Taki, S.; Kadotani, T.; Kai, S. *J. Phys. Soc. Jpn.* **1999**, *68*, 1286−1291. Hibino, M.; Sumi, A.; Tsuchiya, H.; Hatta, I. *J. Phys. Chem. B* **1998**, *102*, 4544−4547. Fang, H. B.; Giancarlo, L. C.; Flynn, G. W. *J. Phys. Chem. B* **1998**, *102*, 7421−7424. Plass, K. E.; Kim, K.; Matzger, A. J. *J. Am. Chem. Soc.* **2004**, *126*, 9042−9053. Wei, Y. H.; Kannappan, K.; Flynn, G. W.; Zimmt, M. B. *J. Am. Chem. Soc.* **2004**, *126*, 5318−5322.
(26) Fey, T.; Holscher, M.; Keul, H.; Hocker, H. *Polym. Int.* **2003**, *52*, 1625−1632.
(27) Hirano, H.; Watase, S.; Tanaka, M. *J. Appl. Polym. Sci.* **2004**, *91*, 1865−1872.
(28) Tsai, C. J.; Chen, Y. *J. Polym. Sci. Polym. Chem.* **2002**, *40*, 293−301.
(29) Mizuno, M.; Hirai, A.; Matsuzawa, H.; Endo, K.; Suhara, M.; Kenmotsu, M.; Han, C. D. *Macromolecules* **2002**, *35*, 2595−2601.
(30) Neffgen, S.; Kusan, J.; Fey, T.; Keul, H.; Hocker, H. *Macromol. Chem. Phys.* **2000**, *201*, 2108−2114. Myrvold, B. O.; Kondo, K.; O'Hara, S. *Mol. Cryst. Liq. Cryst. Sci. Technol., Sect. A* **1995**, *269*, 99−110. Tamaoki, N.; Kruk, G.; Matsuda, H. *J. Mater. Chem.* **1999**, *9*, 2381−2384.

Table 2. Lattice Energies of the Periodic Models of Alkyl Dicarbamates Computed by the COMPASS Force Field (kcal/mol)[a]

	dicarbamate		
	8-8-8	**8-9-8**	**8-12-8**
lattice energy	−28.4	−26.5	−30.2
van der Waals term	−15.3	−16.0	−17.0
electrostatic term	−13.1	−10.8	−13.1

[a] These values represent the energy obtained by the formation of the periodic assembly from isolated single molecules.

even-numbered alkyl dicarbamates, which possess an anti conformation, neighboring molecules in a molecular column can slip to find an optimal hydrogen-bonding geometry for both carbamate functional groups (Figure 5). However, this is not possible for odd-numbered alkyl dicarbamates, which have a syn geometry, because offsetting molecules gives rise to different geometries for the two carbamate functional groups and repulsive interactions between alkyl chains. This effect is manifested in the crystal structures of **8-4-8** and **8-5-8 dicarbamates**. The odd-numbered **8-5-8 dicarbamate** has a nearly 90° angle (89.7°) between the central alkyl chain and the molecular column direction, whereas in the even analogue (**8-4-8 dicarbamate**) this angle is not 90° but rather 86.3°.

Competitive Monolayer Formation. The STM images discussed above illustrate the structure of the interfacial layer when only one dicarbamate is present. However, industrial coating solutions often consist of mixtures. In these cases competitive adsorption between multiple adsorbates determines the composition of the interfacial layer. Previous studies of competitive adsorption at the liquid−solid interface revealed that, in general, the longer molecule in the mixture preferentially adsorbs onto the surface.[31] Although these studies employed calorimetry,[32] neutron diffraction, differential scanning calorimetry,[31,33] and STM, the high spatial and fast temporal resolution offered by STM makes it a unique tool to study competitive monolayer formation with direct observation of monolayer structure.

The STM image in Figure 6a shows the structure of the monolayer formed from a 1:1 molar mixture of **8-12-8** and **8-9-8 dicarbamates**. The molecular geometry observed from the STM image clearly shows the anti conformation of the two terminal alkyl chains demonstrating that the imaged area is entirely composed of **8-12-8 dicarbamate**. Consistent with this observation is the 4.4 nm column width observed in multiple domains which is identical to that in pure monolayers of **8-12-8 dicarbamate**. STM imaging of mixtures containing higher mole fractions (>0.5) of **8-12-8 dicarbamate** consistently resulted in the formation of the monolayer entirely composed of the longer adsorbate.

Increasing the mole fraction of **8-9-8 dicarbamate** (and lowering the mole fraction of **8-12-8 dicarbamate**) gave rise to a change in the monolayer composition. The STM image in Figure 6b is obtained from a mixture containing 0.3 mole fraction of **8-12-8 dicarbamate** and is composed of **8-9-8 dicarbamate** as evidenced by the syn conformation of the two terminal alkyl chains. This molecular geometry combined with the measured column width of 4.0 nm demonstrates that the entire monolayer is composed of **8-9-8 dicarbamate**.

At intermediate mole fractions, the coexistence of **8-9-8** and **8-12-8 dicarbamates** is observed. For example, a mixture containing 0.44 mole fraction of **8-12-8 dicarbamate** shows coexistence of separate **8-9-8** and **8-12-8 dicarbamate** domains (Figure 6c). In general, when the monolayer is composed of both alkyl dicarbamates, phase separation is observed.[34] In a few cases, side-by-side arrangement of two alkyl dicarbamates instead of complete segregation in the monolayer occurs (Figure 6d). STM imaging of mixtures of varying molar ratios of **8-9-8** and **8-12-8 dicarbamates** indicated that the mixed monolayer is formed when the mole fraction of **8-12-8 dicarbamate** is in the range 0.35(1)−0.48(1).

In the case of the mixture of **8-8-8** and **8-12-8 dicarbamates**, both alkyl dicarbamates have an anti geometry between the two terminal alkyl chains. Because the resolution of **8-8-8 dicarbamate** monolayers was generally poor, identification of monolayer composition in competition experiments was based on the column width: 3.8(3) nm for **8-8-8 dicarbamate** compared to 4.4(2) nm for **8-12-8 dicarbamate**. Mixtures of **8-8-8** and **8-12-8 dicarbamates** provided a monolayer composed of both molecules when the mole fraction of **8-12-8 dicarbamate** was 0.40(1)−0.47(1). Higher mole fractions of **8-12-8 dicarbamate** provided monolayers composed exclusively of this adsorbate, whereas lower mole fractions gave rise to **8-8-8 dicarbamate** monolayers.

In each of the competitive adsorption experiments, the composition of the monolayer showed marked dependence on the relative mole fraction of each alkyl dicarbamate in solution. The STM experiments were performed in dilute solutions and the molecules adsorbed are in dynamic equilibrium. The equilibrium constant of this process is related to the concentration of each adsorbate in the solution and the fractional surface coverage by the following equation.[35] Applying the Langmuir model for two adsorbates,

$$\frac{\theta_1}{\theta_2} = \frac{K_1 a_1}{K_2 a_2} \tag{1}$$

where θ is the fractional surface coverage of each adsorbate, K is the equilibrium constant for the adsorption from the solution onto the surface, and a is the activity of each molecule in the solution. The equilibrium constant is related to the free energy change associated with the process by

$$\frac{K_1}{K_2} = \frac{e^{(-\Delta G_1/RT)}}{e^{(-\Delta G_2/RT)}} = e^{-(\Delta G_1 - \Delta G_2)/RT} \tag{2}$$

(31) Castro, M. A.; Clarke, S. M.; Inaba, A.; Thomas, R. K.; Arnold, T. *J. Phys. Chem. B* **2001**, *105*, 8577−8582.
(32) Findenegg, G. H.; Liphard, M. *Carbon* **1987**, *25*, 119−128.
(33) Castro, M. A.; Clarke, S. M.; Inaba, A.; Arnold, T.; Thomas, R. K. *J. Phys. Chem. B* **1998**, *102*, 10528−10534.
(34) Phase separation is typically observed in competitive adsorption of two molecules that are significantly different in packing geometry. This phenomenon results from the loss of intermolecular interaction when two different adsorbates are neighboring in a molecular column. By contrast, if the two adsorbates possess very similar packing structures, random mixing occurs. See: Yablon, D. G.; Ertas, D.; Fang, H. B.; Flynn, G. W. *Isr. J. Chem*. **2003**, *43*, 383−392. Stevens, F.; Beebe, T. P. *Langmuir* **1999**, *15*, 6884−6889. Yablon, D. G.; Wintgens, D.; Flynn, G. W. *J. Phys. Chem. B* **2002**, *106*, 5470−5475. Gesquière, A.; De Feyter, S.; De Schryver, F. C.; Schoonbeek, F.; van Esch, J.; Kellogg, R. M.; Feringa, B. L. *Nano Lett*. **2001**, *1*, 201−206. Cousty, J.; Van, L. P. *Phys. Chem. Chem. Phys*. **2003**, *5*, 599−603. Padowitz, D. F.; Messmore, B. W. *J. Phys. Chem. B* **2000**, *104*, 9943−9946. Ohshiro, T.; Ito, T.; Buhlmann, P.; Umezawa, Y. *Anal. Chem*. **2001**, *73*, 878−883.
(35) Venkataraman, B.; Breen, J. J.; Flynn, G. W. *J. Phys. Chem.* **1995**, *99*, 6608−6619.

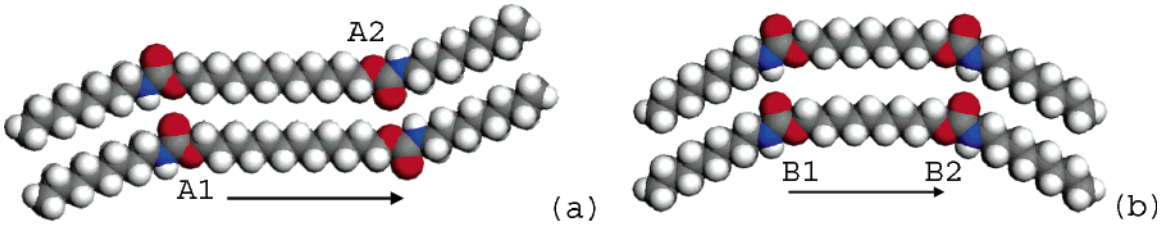

Figure 5. Molecular models demonstrating the odd−even effect on hydrogen-bonding geometry. (a) Upon slipping the lower molecule along the arrow direction, the two N−H···O═C hydrogen bonds (A1 and A2) move in the same relative direction in **8-12-8 dicarbamate**, providing an equivalent hydrogen-bonding environment for A1 and A2. (b) However, the same modification gives rise to nonequivalent geometries for the two N−H···O═C hydrogen bonds (B1 and B2) in **8-9-8 dicarbamate**. Therefore, slipping of the molecule enhances one hydrogen bond while weakening the other.

The ΔG in this case is the change of free energy associated with monolayer formation. For competition between **8-9-8** and **8-12-8 dicarbamates**, solutions composed of 0.35(1)−0.48(1) mole fraction of **8-12-8 dicarbamate** produced mixed monolayers. In this range there is a condition that the surface concentration of the two adsorbates becomes equal. At this point, $\theta_1 = \theta_2$. Therefore,

$$\frac{K_1 a_1}{K_2 a_2} = 1 \quad \text{and} \quad \frac{K_1}{K_2} = e^{-(\Delta G_1 - \Delta G_2)/RT} = e^{\Delta(\Delta G)/RT} = \frac{a_2}{a_1} \qquad (3)$$

The terms a_1 and a_2 can be replaced by the mole fraction of each alkyl dicarbamate in the dilute solution limit.[35] Therefore, $\Delta(\Delta G)$ is between 0.37(2) and 0.05(2) kcal/mol for this process, in which ΔG for adsorption of **8-12-8 dicarbamate** is more favorable than for **8-9-8 dicarbamate**. Applying this analysis to mixtures of **8-8-8** and **8-12-8 dicarbamates** finds that $\Delta(\Delta G)$ is between 0.24(2) and 0.07(2) kcal/mol and that ΔG of adsorption for **8-12-8 dicarbamate** is larger. The $\Delta(\Delta G)$ between **8-8-8** and **8-9-8 dicarbamates** was not obtained directly because of the experimental difficulty associated with assigning domain composition.[36] This value may be estimated, however, on the basis of the competition experiment of the two dicarbamates with **8-12-8 dicarbamate**, with the assumption that the change of surface composition is symmetric within the mole fraction range that produces mixed monolayers. In this case $\Delta(\Delta G)$ is at the center of the estimated range; $\Delta(\Delta G)$ between **8-8-8** and **8-12-8 dicarbamates** is 0.16(3) kcal/mol and $\Delta(\Delta G)$ between **8-9-8** and **8-12-8 dicarbamates** is 0.21(3) kcal/mol. Based on these values, $\Delta(\Delta G)$ between **8-8-8** and **8-9-8 dicarbamates** is 0.05(4) kcal/mol, indicating that there is no significant difference in ΔG of adsorption between these two alkyl dicarbamates.[37]

For mixtures of *n*-alkanes, it is found that longer molecules preferentially adsorb on the substrate[38] even when the mole fraction of the longer alkane is significantly lower than that of the shorter alkane.[39] For example, a mixture of *n*-octane and *n*-decane produces a monolayer exclusively composed of the longer adsorbate with a 0.28 mole fraction of *n*-decane.[31] In contrast, complete coverage by *n*-octane is achieved only when the mole fraction of this molecule is close to 1. This preference for adsorption of the longer molecule is also found when the length of the alkanes differ by only one carbon.[33] A plausible explanation for this phenomenon is provided by considering the entropy change of the system. Fewer molecules are required to fill a given surface area of the substrate when the longer molecule forms the monolayer, resulting in a smaller entropic penalty. In this study, the mixture of alkyl dicarbamates also formed a monolayer of the longer alkyl dicarbamate from a 1:1 solution of a long and a short molecule. However, the preference for the longer molecule is significantly reduced, despite the fact that the shorter dicarbamates are approximately 3-fold more soluble in phenyloctane. One possible explanation for the relative preference of shorter molecules for alkyl dicarbamate monolayers compared to *n*-alkanes is the existence of dense hydrogen bonding in the former. Each alkyl dicarbamate can participate in four hydrogen bonds. If the shorter molecule constitutes the monolayer, a greater number of hydrogen bonds are formed within the monolayer because its unit cell occupies a smaller surface area compared to the longer dicarbamate. Hydrogen bonding is stronger than van der Waals interaction on a per occupied unit surface area basis and accordingly the total intermolecular interaction obtained by forming the monolayer is greater when a smaller alkyl dicarbamate forms a monolayer. This is exemplified by comparing two-dimensional lattice energies of **8-8-8** and **8-12-8 dicarbamates**. As expected the lattice energy of **8-12-8 dicarbamate** (−30.2 kcal/mol) is greater than that of **8-8-8 dicarbamate** (−28.4 kcal/mol) on a per molecule basis. However, this order is reversed when they are compared on a per unit area basis. Employing unit cell parameters obtained by computation, the lattice energies are −7.8 kcal/nm^2 for **8-8-8 dicarbamate** and −7.3 kcal/nm^2 for **8-12-8 dicarbamate**, indicating a greater stabilization for **8-8-8 dicarbamate**. This is a manifestation of the higher hydrogen-bonding density in the latter. Therefore, through intermolecular interaction in the monolayer alone, a shorter alkyl dicarbamate is preferred to form the monolayer. Opposing this effect, and favoring the adsorption of **8-12-8 dicarbamate**, is the change of entropy, which favors adsorbing a smaller number of molecules on the surface. This situation arises because the surface area of the substrate is the limiting factor determining number of adsorbed molecules rather than the availability of

(36) The STM images of both **8-9-8** and **8-8-8 dicarbamates** generally exhibited low resolution and their column widths are too close to unambiguously assign the monolayer composition on the basis of the column width alone. Repeated STM experiments on the mixture of the two alkyl dicarbamates in various mole fractions did not provide reliable data on the monolayer composition. Because of the difficulty associated with obtaining conclusive data, competitive monolayer formation between **8-9-8** and **8-8-8 dicarbamates** was not further pursued.

(37) That there is no significant difference in ΔG of monolayer formation between **8-8-8** and **8-9-8 dicarbamates** was not predicted computationally (see Table 2). This may indicate an inadequacy in the computational method employed or signal that comparison with isolated single molecules is not valid in this case. Furthermore, the relative entropic changes are not included in the computation and may not be similar for the two carbamates.

(38) Aveyard, R. *Trans. Faraday Soc.* **1967**, *63*, 2778−2788. Smith, P.; Lynden-Bell, R. M.; Smith, W. *Mol. Phys.* **2000**, *98*, 255−260. Xia, T. K.; Landman, U. *Science* **1993**, *261*, 1310−1312.

(39) This trend is also found in carboxylic acids. See: Yablon, D. G.; Ertas, D.; Fang, H. B.; Flynn, G. W. *Isr. J. Chem.* **2003**, *43*, 383−392.

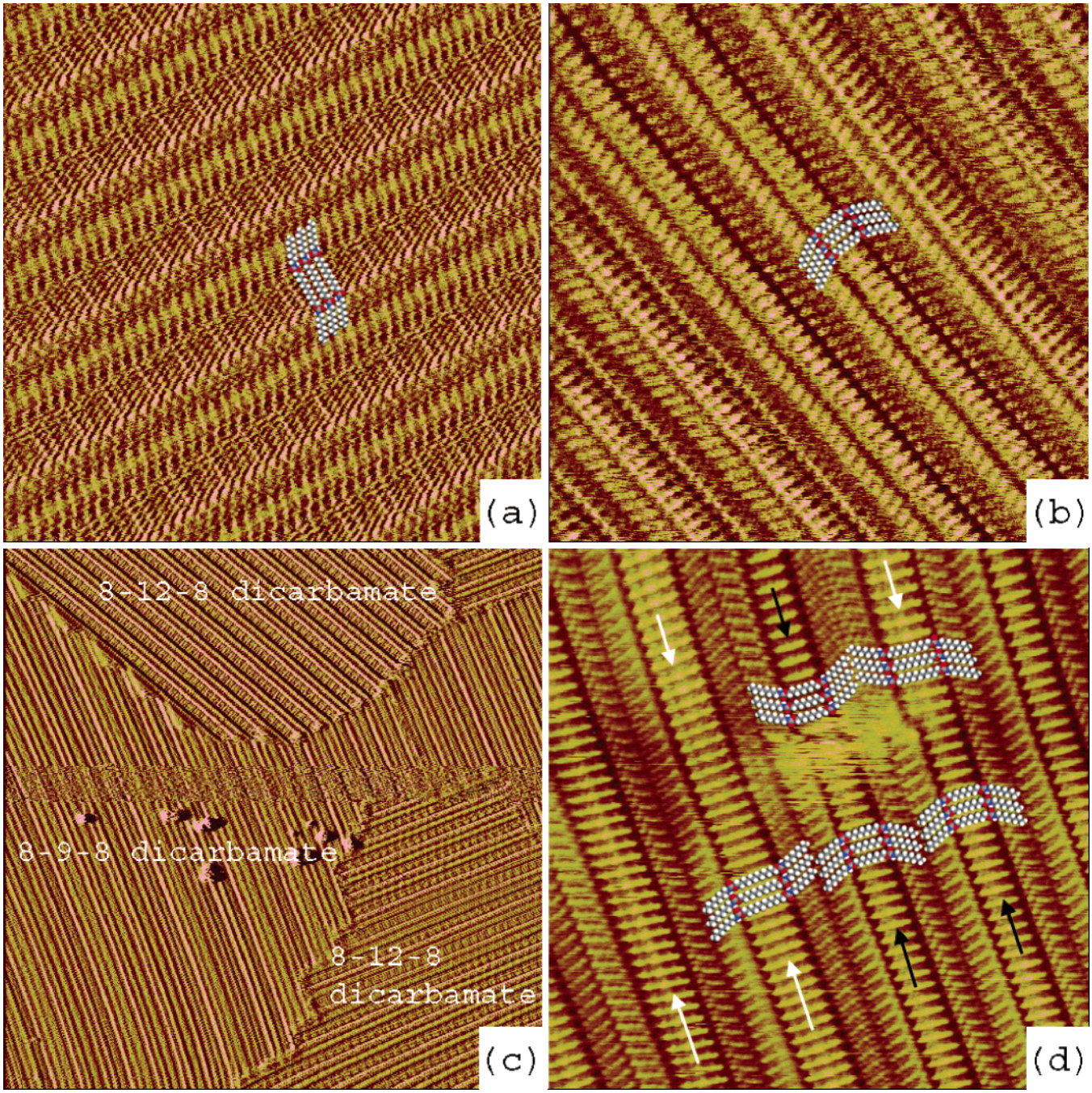

Figure 6. STM images obtained by competitive adsorption between **8-9-8** and **8-12-8 dicarbamates** in various mole fractions. (a) STM image (20 × 20 nm^2) showing an **8-12-8 dicarbamate** monolayer (mole fraction of **8-12-8 dicarbamate** = 0.5). (b) STM image (20 × 20 nm^2) displaying an **8-9-8 dicarbamate** monolayer (mole fraction of **8-12-8 dicarbamate** = 0.3). (c) STM image (100 × 100 nm^2) demonstrating phase separation of **8-9-8** and **8-12-8 dicarbamates** (mole fraction of **8-12-8 dicarbamate** = 0.44). (d) STM image (20 × 20 nm^2) showing neighboring molecular columns of **8-12-8** and **8-9-8 dicarbamates**. White and black arrows denote molecular columns of **8-12-8** and **8-9-8 dicarbamates**, respectively (mole fraction of **8-12-8 dicarbamate** = 0.35).

molecules for adsorption. This is also the case for most coating applications and therefore this factor must be considered when predicting the composition of an interfacial layer produced from a mixture of adsorbates.

Conclusion

The packing structures of alkyl dicarbamates in two- and three-dimensional crystals were revealed by STM imaging and X-ray structure determination. The physisorbed monolayers and three-dimensional crystals demonstrated isostructural packing as well as variation of molecular geometry by the odd−even effect. In addition, the variation of melting points proved that the change in intermolecular interaction due to the modification of the packing geometry has a dramatic effect on physical properties. This correlation supports the notion of employing physisorbed self-assembled monolayers as a model system for engineering solid-state materials for surface coating applications. Competitive monolayer formation from mixtures of two different alkyl dicarbamates showed the variation of monolayer composition depending on the solution composition of each molecule.

Although the longer alkyl dicarbamate is preferred to form the monolayer, compared to *n*-alkanes the preference for adsorbing the longer molecule is reduced significantly. This change arises from the existence of hydrogen bonds in the monolayer that increase energetically favorable intermolecular interactions for a smaller molecule on a per unit area basis.

Acknowledgment. This work was supported by the National Science Foundation under grant CHE-0316250.

Supporting Information Available: Detailed synthetic procedures and characterization for each alkyl dicarbamate; full details of the X-ray structure determination; X-ray crystallographic data (in CIF format) and ORTEP diagrams of **8-4-8** and **8-5-8 dicarbamate**. This material is available free of charge via the Internet at http://pubs.acs.org.

JA043028+